1971

Optimum fracture toughness of fiber-reinforced composites

Paul S. Shenberger
Lehigh University

OPTIMUM FRACTURE TOUGHNESS OF FIBER-REINFORCED COMPOSITES

BY

PAUL S. SHENBERGER

ABSTRACT

The effects of reinforcing fibers on the fracture toughness, critical stress intensity factor, and Young's modulus of an epoxy resin are investigated. By varying the volume percentage of glass fibers oriented parallel to a crack, it is found that there exists an optimum fracture toughness of the composite dependent upon the fiber volume percentage and the constituents of the composite. The simple relationship between k_c, the critical stress intensity factor, and G_c, the crack toughness, for a homogeneous material in the linear elastic theory of fracture mechanics is found to hold with reasonable accuracy for the case of a crack extending parallel to the fibers when equivalent elastic constants for the composite system are used in the calculation.

It is also shown that the use of graphite fibers in the same resin matrix results in lower values of k_c and G_c than those for glass fibers. The increased resistance to crack growth of composites with fibers oriented at an angle with the preferred direction of crack growth is also demonstrated.

OPTIMUM FRACTURE TOUGHNESS OF FIBER-REINFORCED COMPOSITES

BY

PAUL S. SHENBERGER

A Thesis
Presented to the Graduate Committee
of Lehigh University
in Candidacy for the Degree of
Master of Science
in
Applied Mechanics

LEHIGH UNIVERSITY

1971

This thesis is accepted and approved in partial fulfillment of the requirements for the degree of Master of Science.

August 30, 1971
(date)

George C. Sih
Professor in Charge

Ferdinand P. Beer
Chairman of Department

ACKNOWLEDGEMENTS

The author wishes to express his appreciation to Professor George C. Sih for his invaluable guidance in the preparation of this thesis. Sincere thanks are also due to Dr. Robert P. Wei and Mr. Jack Fitzgerald for their assistance in the experimental work involved and to Mrs. Carol Beigel who typed the thesis.

Samples for the testing program were furnished by the Air Force Materials Laboratory through the University of Dayton.

TABLE OF CONTENTS

LIST OF FIGURES

LIST OF TABLES

ABSTRACT

The effects of reinforcing fibers on the fracture toughness, critical stress intensity factor, and Young's modulus of an epoxy resin are investigated. By varying the volume percentage of glass fibers oriented parallel to a crack, it is found that there exists an optimum fracture toughness of the composite dependent upon the fiber volume percentage and the constituents of the composite. The simple relationship between k_c, the critical stress intensity factor, and G_c, the crack toughness, for a homogeneous material in the linear elastic theory of fracture mechanics is found to hold with reasonable accuracy for the case of a crack extending parallel to the fibers when equivalent elastic constants for the composite system are used in the calculation.

It is also shown that the use of graphite fibers in the same resin matrix results in lower values of k_c and G_c than those for glass fibers. The increased resistance to crack growth of composites with fibers oriented at an angle with the preferred direction of crack growth is also demonstrated.

I. INTRODUCTION

A great deal of interest has been focused recently on the area of high strength fibers and composites of these fibers embedded in a supporting matrix material. The advantages of the high strength to weight ratio of such composites are obvious for engineering applications and have been widely discussed.

Considerable work [1-4][1] has already been done in finding equivalent elastic constants for such materials. As with any engineering material it is also necessary to have some knowledge of the fracture mechanics of these composite systems. Rosen [5] has characterized the modes of failure in composite materials. Hertzberg, et al, [6] and Sih, et al, [7,8] have reported the work carried out at Lehigh in the area of fracture of composites. This thesis presents the results of experimental testing being done to compliment the analytic study of crack problems in composites.

The main thrust of this experimental work is to determine if there is an optimum volume fraction of fibers in a composite for resisting crack propagation parallel to those fibers. A peak in the fracture toughness is expected from the results of Sih, et al, [8] and Parikh [9] who reported

[1] Numbers in brackets refer to references on page.

evidence of decreasing fracture energies with increasing fiber volume fraction in silver matrix, steel fiber composites. It is also desired to test whether the simple relationship between the critical crack tip stress intensity factor, k_c, and the fracture toughness, G_c, for a homogeneous material in the linear elastic theory of fracture mechanics holds for a composite system using equivalent elastic constants.

Tests are to be conducted which show the effects of E-glass vs. graphite, Thornel 50, fibers on the fracture characteristics. The crack resisting property of fibers not parallel to the preferred crack direction and the relationship between the crack growth rate and the crack extension driving force will also be investigated.

II. TESTING PROGRAM

A. APPLICATION OF FRACTURE MECHANICS TESTING TO COMPOSITES

Techniques of crack toughness measurements of sheet metals have been well developed in the field of fracture mechanics. The results of the preliminary analytical analysis indicate that the concept of fracture mechanics may be applied to classify the strength of composite materials [7]. That is the stress field close to the end of a crack in a composite can be characterized by a single stress-field parameter k, the stress-intensity factor. There is thus a value of k corresponding to each pair of values of the load and crack size at any stage of a test. As the load is increased from zero, the crack length at first changes imperceptibly and then more and more rapidly until a point is reached at which the rate of crack extension increases abruptly. This abrupt change from slow to fast crack propagation is a critical point in the fracturing process. The value of k at this point, termed k_c, provided a useful measure of the resistance to crack propagation or alternatively the crack strength.[2] It should be pointed out that the crack strength materials property of the composite

---

[2] k_c, the critical stress intensity factor, is here considered to be a measure of crack strength. G_c, the critical energy release rate or crack driving force, is considered to be a measure of the crack toughness of the material.

k_c is not the same thing as the stress-field parameter k obtained analytically, although they are equal to each other at the critical point of crack instability. The resistance to crack growth can also be characterized by G, the crack extension driving force, and the resistance to unstable crack growth by G_c, the critical crack extension driving force or fracture toughness.

B. TEST SPECIMENS

The tests employ compact-tension specimens as shown in Figure 1 and discussed by Brown and Srawley [10]. These specimens are essentially edge-notched and edge-loaded specimens furnished by the Air Force Materials Laboratory. The composite materials tested include samples of the epoxy resin matrix ERL-2256/ZZL0820 and samples of the matrix in which unidirectional E-glass or Thornel 50-graphite fibers are embedded. Two samples of laminated graphite fibers with fiber orientation ±60° to the crack direction in addition to layers aligned with the crack were also tested. The following table shows letter designations and their corresponding fiber orientation, fiber volume fraction, and fiber material.

TABLE 1

TYPE	FIBER ORIENTATION	FIBER MATERIAL	FIBER VOLUME PERCENT
E	none		0
N	Parallel to crack 0°	Glass	10
A	"	Glass	20
H	"	Glass	50
B	"	Glass	60
T	"	Graphite	50-55
S	Laminated 0°, ±60° 12 layers each	Graphite	50-55

C. COMPLIANCE MEASUREMENT

This test is designed to determine the G_c-value of a cracked specimen by direct measurement of the displacement of certain gage length L for varying lengths of cracks and at different critical loads P. For a compact tension specimen, L corresponds to the distance between the applied loads P and the displacement of the load points is therefore the changed length ΔL (see Figure 1). This gives the rate of change of $\Delta L/P$ with the crack length a and hence [11]

$$G = \frac{1}{2B} P^2 \frac{\partial(\Delta L/P)}{\partial a} \qquad (1)$$

can be computed at fracture giving G_c. The quantity $\Delta L/P$ is called the "compliance" of the specimen, and B represents the thickness of the specimen.

To carry out the compliance test, a 2000 lb. capacity Tensometer load frame was used. A greater accuracy was achieved in the load range of 100 lb. by using a Bytrex LD-100 load cell mounted between the sample grip and the movable Tensometer head as shown in Figure 2. Displacements were measured using a G.L. Collins transducer mounted on the grips of the Tensometer. The outputs from the load cell and transducer were fed through the Micro Strain and Full Stroke modules of an MTS control console. The outputs are plotted by a Varian X-Y recorder as a load-displacement curve.

The true load-displacement relation for the cracked composite specimen is obtained by first determining the deflection of the system using an aluminum block. The resulting load-displacement curve was then subtracted graphically from that obtained from the composite specimen for the correction. This resulted in a linear curve from which $\Delta L/P$ was obtained.

Notches of increasing length were cut into the samples with a jeweler's saw in approximately 0.1 inch increments. Crack lengths were measured using a travelling microscope.

Readings were obtained for crack lengths up to approximately 1.70 inches for most materials. To prevent premature failure of the specimens at the longer crack lengths, it was necessary to progressively reduce the maximum load for crack length a>.60 inches. Three runs were initially made at each crack length. It was found that after the first three runs at a given crack length each subsequent run yielded an identical curve. After the first few crack lengths the curves were identical starting with the second and only two runs were made at each crack length. The second run at each crack length was regarded as a reliable measure of $\Delta L/P$ since the variation between the second and all subsequent runs never exceeded two percent.

Loads were applied only by the pins through the holes in the specimens, and only along the axis of the Tensometer. The grips of the Tensometer which normally pivoted in ball and socket joints had been aligned and shimmed rigid under 1500 lbs. of tension. Therefore the specimens were not clamped in the grips, thus insuring that no twisting load was applied. This technique was necessary to insure the alignment of the transducer which was clamped to the grips.

Figures 4 through 12 show the compliance plotted vs. a/W where a is the crack length and W the specimen width as defined in Figure 1. Curves drawn through the data points represent least squares fits to fifth order polyno-

mials. Specimen types A and B represent samples provided for previous testing [7] and one sample of each which was tested to corroborate those results. These tests show greater data scatter and results were not obtained for crack lengths as long as for the other samples.

The quantity $\partial(\Delta L/P)/\partial a$ was obtained by differentiating the polynomial approximations to the data curves for all but the A samples for which the curve fit was not sufficiently smooth. Critical values of P and a were obtained from fracture tests outlined in the following section.

D. CRITICAL VALUES OF STRESS INTENSITY FACTOR

Fracture tests were run on the same experimental set up that was described in Section C for compliance measurement. The idea here is to measure critical values of the load P and crack length a at the point of unstable crack extension so that the stress-intensity factor as derived from the linear theory of elasticity [10]

$$k = Y\left(\frac{a}{W}\right) \frac{P\sqrt{a}}{BW\sqrt{\pi}} \qquad (2)$$

can be calculated. In the above equation, Y(a/W) is a function depending upon the ratio of the crack length to the width of the specimen W. Values for Y were obtained from [10].

Results were recorded from three different types of tests as follows:

(1) Data were obtained from specimens which experienced unstable crack growth during the compliance tests. These specimens contained pre-cut "cracks" whose tips were not very sharp.

(2) These specimens were specially prepared for the fracture tests by precracking the specimens under cyclic loading and then broken in static tension.

(3) Specimens which had previously undergone unstable crack growth were also retested.

The last two types of test specimens involved reasonably sharp crack tips and a comparison of results from the two types of crack tip provided some insight into the effects of crack tip radius on the measured parameters.

E. FRACTURE TEST FOR LAMINATED SAMPLE

The fracture test for the laminated sample differed in that it had to be carried out on the 100,000 lb. capacity MTS testing machine. This was necessary since it was the only sample that would not break within the 100 lb. range of the Bytrex load cell at a reasonable crack length. The MTS load cell was used to moniter load and a clip gauge to measure the displacement. The remainder of the system remained the same as for the compliance testing.

III. TEST RESULTS

A. RELATIONSHIP OF FRACTURE TOUGHNESS VALUE AND CRITICAL STRESS-INTENSITY FACTOR

Since the precise relationship between the strain energy release rate G and the stress-intensity factor k of a heterogeneous system such as the fiber reinforced composite is not known and cannot be easily obtained analytically, it would be informative to investigate the possibility of using the well-known expression

$$G_c = \frac{k_c^2}{E_{eff}} (1 - \nu_{eff}) \qquad \text{(Plane Strain)} \qquad (3)$$

derived for a homogeneous and isotropic system. In eq.(3) the Young's modulus E and Poisson's ratio ν are replaced by E_{eff} and ν_{eff} representing the effective quantities for the entire composite body. Keeping in mind here that both E_{eff} and ν_{eff} depend on the fiber volume fraction of the composite.

First, the Young's modulus of the composite for each fiber volume fraction (ranging from 0% to 60%) was found by multiplying the ratio of the compliance for that fiber volume to that of the matrix material by the Young's modulus for the matrix material. This ratio was found to be constant within five percent at any crack length. Figure 13 compares the values obtained to those of Chen and Lin [4]. The Poisson's ratio ν_{eff} was estimated from

the known values for the matrix material 0.35 and the fiber material 0.20 for glass and from the results of Adams and Doner [1]. Similar tests were performed on the graphite fiber composite. The results are shown in Table 2 for the glass fiber and Table 3 for the graphite fiber. The graphite A data represents samples with cut notches and the B data samples with sharp cracks. The dependence of G_c and k_c on crack sharpness was obvious for graphite specimens but not for glass specimens. The C data is for the laminated specimens.

Values of $G_c^{(2)}$ were found using the technique described in Section III.C. The crack length, compliance, and critical load were measured during the tests. Figures 14 through 17 compare the compliance values for the fracture specimens to the compliance calibration curves for the various fiber volume fractions. Fracture results which did not fall on the calibration curve were corrected to the curve by assuming that the compliance measurement was the correct one and the corresponding crack length and slope were found from the calibration curve. It was found that points which differed greatly from the compliance curves resulted from retests of previous fracture specimens. The errant points occurred when the unstable crack growth in the previous test was not enough for the load to drop off more than one or two pounds. Points resulting from such tests were then dropped from the data.

Values of $G_c^{(2)}$ with the superscript (2) signify the energy release rate obtained directly from the compliance measurement technique as described in Section II.C. and hence $k_c^{(2)}$ is calculated indirectly using eq.(3). On the other hand $k_c^{(1)}$ with the superscript (1) is found from a fracture test in II.D. and $G_c^{(1)}$ is computed from eq.(3). All these are average values for their respective fiber volume fractions. The percentage of deviation compares the experimentally measured values of G_c and k_c using eqs.(1) and (2). The objective is to check whether eq.(3) will then represent the relationship between k_c and G_c for a fiber reinforced composite. The deviation is based on the value which was found more directly, i.e.,

$$G_c\text{-\% deviation} = \frac{G_c^{(2)} - G_c^{(1)}}{G_c^{(2)}} \times 100\% \qquad (4a)$$

$$k_c\text{-\% deviation} = \frac{k_c^{(1)} - k_c^{(2)}}{k_c^{(1)}} \times 100\% \qquad (4b)$$

Note that the percent of deviation for the glass fiber composite is no more than 3% on k_c and approximately 6% on G_c. This means that the compact tension specimen with an edge crack has determined the fracture toughness value of the composite pulling normal to the fibers with good accuracy. The deviations on the graphite fiber composite were appreciable and the data in Table 3 collected from the edge-

TABLE 2. GLASS FIBER SAMPLES

Volume Fraction %	Fracture		Compliance		ν_{eff}	E_{eff} x 10^6 psi	% Deviation	
	$G_c^{(1)}$ lb-in/in^2	$k_c^{(1)}$ lb/in$^{3/2}$	$G_c^{(2)}$ lb-in/in^2	$k_c^{(2)}$ lb/in$^{3/2}$			G_c	k_c
0	0.76	373	0.77	374	0.35	0.50	+1.3	-0.4
10	3.02	1,020	2.98	1,000	0.33	0.95	-1.3	+1.1
20	2.62	965	2.47	935	0.32	1.00	-6.1	+2.9
50-55	2.28	1,090	2.31	1,100	0.30	1.50	+1.3	-0.5
60	1.78	1,100	1.81	1,120	0.29	2.00	+3.9	-2.0

TABLE 3. GRAPHITE FIBER SAMPLES

Volume Fraction %	Fracture		Compliance		ν_{eff}	E_{eff} x 10^6 psi	% Deviation	
	$G_c^{(1)}$ lb-in/in^2	$k_c^{(1)}$ lb/in$^{3/2}$	$G_c^{(2)}$ lb-in/in^2	$k_c^{(2)}$ lb/in$^{3/2}$			G_c	k_c
0	0.76	373	0.77	374	0.35	0.50	+1.3	-0.4
50-55A	1.34	765	0.84	603	0.30	1.25	-60	+21
50-55B	0.40	413	0.24	328	0.30	1.25	-65	+21
50-55C	55	2.1×10^4	160	3.6×10^4	0.30	7.5	+65	-70

notched specimen are not representative of the fracture mode of the composite. In fact, it was observed during the tests that the graphite composite resulted in a substantial amount of debonding or separation of the fibers from the matrix. Hence, a considerable amount of free surface is created through fiber separation, which is not accounted for in eq.(2) for the computation of k_c. A different specimen would have to be used for determining the fracture toughness of the graphite composite or a more refined analysis of the problem including fiber debonding would have to be made.

B. ORTHOTROPIC MODEL

It is possible to examine the relationship between G_c and k_c for an anisotropic material in addition to the previous technique of using a homogeneous isotropic material with equivalent elastic constants. Sih and Liebowitz [11] obtained a relationship between G_1 and k_1 for a generally anisotropic material in which the direction of crack propagation is collinear with the original crack and the crack is opened by a constant surface pressure. For this case the system is said to be orthotopic and the resultant relationship is

$$G_1 = \pi k_1^2 \left(\frac{a_{11}a_{22}}{2}\right)^{\frac{1}{2}} \left[\left(\frac{a_{22}}{a_{11}}\right)^{\frac{1}{2}} + \frac{2a_{12} + a_{66}}{2a_{11}}\right]^{\frac{1}{2}}$$

where the elastic coefficients, a_{ij}, are related to the principle elastic constants as follows:

$$a_{11} = \frac{1}{E_1}, \quad a_{22} = \frac{1}{E_2}, \quad a_{12} = \frac{-\nu_{12}}{E_1}, \quad a_{66} = \frac{1}{\mu_{12}}$$

Using the values of the principle elastic constants furnished by the Air Force Materials Lab, values were obtained for $G_c^{(1)}$ and $k_c^{(2)}$ as in Tables 2 and 3. Tables 4 and 5 present the results for the orthotropic case.

Comparing Tables 2 and 3 with Tables 4 and 5 shows that the orthotropic representation generally is not as good as the isotropic model. The percentage deviation is slightly lower for the unidirectional graphite samples but not significantly. The orthotropic representation provides a poor model for the glass samples, particularly in the lower volume fractions. It is expected that as the volume fraction increases the material will become more anisotropic and the orthotropic model offers a better prediction. This trend is verified in Table 4.

It can be concluded that the isotropic model using equivalent elastic constants provided the best model for the experimental glass samples for all volume fractions. The orthotropic model provided a representation which became reasonable for volume fractions over 50%. Neither

TABLE 4. GLASS FIBER SAMPLES

Volume Fraction %	Fracture		Compliance		% Deviation		Elastic Constants			
	$G_c^{(1)}$ lb-in/in^2	$k_c^{(1)}$ lb/in$^{3/2}$	$G_c^{(2)}$ lb-in/in^2	$k_c^{(2)}$ lb/in$^{3/2}$	G_c	k_c	E_1 psi x 10^6	E_2 psi x 10^6	ν_{12}	μ_{12} psi x 10^6
0	0.87	373	0.77	350	-13	+6.2	0.50	0.50	.35	.20
10	5.05	1,020	2.98	612	-69	+40	1.51	0.60	.33	.24
20	4.15	965	2.47	745	-68	+23	2.52	0.66	.32	.29
50	2.56	1,090	2.31	1,030	-11	+5.5	5.55	1.33	.28	.54
60	2.04	1,100	1.81	1,070	-13	+2.7	6.56	1.70	.26	.68

TABLE 5. GRAPHITE SAMPLES

Volume Fraction %	Fracture		Compliance		% Deviation		Elastic Constants			
	$G_c^{(1)}$ lb-in/in^2	$k_c^{(1)}$ lb/in$^{3/2}$	$G_c^{(2)}$ lb-in/in^2	$k_c^{(2)}$ lb/in$^{3/2}$	G_c	k_c	E_1 psi x 10^6	E_2 psi s 10^6	ν_{12}	μ_{12} psi x 10^6
0	0.87	373	0.77	350	-13	+6.2	0.50	0.50	0.35	.20
50A	1.28	765	0.84	618	-52	+19	25.2	1.00	0.28	.55
50B	0.37	413	0.24	322	-54	+22	25.2	1.00	0.28	.55

model represented the graphite samples and both resulted in similar descrepancies for the graphite samples. It thus appears that these deviations are due to unaccounted for fracture mechanisms in these samples as mentioned previously.

C. OPTIMUM FRACTURE TOUGHNESS

Figure 18 shows G_c plotted vs. fiber volume fraction for the glass fiber samples. The average found in columns (1) and (2) of the chart is plotted as is the range of values found using both techniques. The 0% data is based on 2 data points, the 10% data on 11 points, the 20% data on 2 points, the 50-55% data on 6 points, and the 60% data on 3 points. The plots indicate the possibility of a crack tip radius dependence for the glass samples since the 20% and 60% data come from specimens with cut notches while the 0%, 10%, and 50-55% were predominately sharp crack tip specimens. This dependence is obviously not as great as for the graphite samples however.

As can be seen from the figure, experimental testing indicates a peak value of G somewhere between 0% and 20% fiber volume. Additional testing would be necessary to locate the actual peak.

Referring to Figure 18, note that the fracture toughness G_c of the glass fiber composite first increases with the fiber volume fraction and then decreases. The peak value of G_c which is approximately three times higher than the fracture toughness of the matrix material occurs at 10 percent volume fraction. This means that in the low fiber volume fraction range the intensity of the load transfer in the high fiber volume fraction range is high, thus lowering the fracture toughness of the composite.

An explanation of this peak phenomenon can be offered by the idealized composite model described by Sih et al. [8] which assumes the matrix material to contain flaws. When the volume fraction of the fibers in a composite is sufficiently low say that the fibers are spaced more than two or three diameters of the fiber apart, the problem can be solved analytically without encountering major difficulties. Since the elastic modulus of the fibers is many times greater than that of the matrix material an increase in the number of the fibers has the effect of reducing the load transfer to the crack tip regions. This increases the fracture toughness of the composite. In the case of a composite with a high fiber volume fraction, many of the fibers are actually in contact with each other causing undesirable high elevation of local stresses. The optimum level of load transfer is achieved when the two opposing effects mentioned

above are balanced. At this point the composite attains its maximum fracture toughness value. Obviously the amount of energy dissipated by the composite material through plastic deformation and other non-linear effects are not accounted for in these simplified models. However, the models do indicate that the geometric arrangement of the fibers can have a strong influence on the strength of the composite.

D. RELATIONSHIP BETWEEN FRACTURE TOUGHNESS AND FIBER MATERIAL AND ORIENTATION

The values for k_c and G_c in Table 2 and 3 indicate that for this particular matrix material and fiber orientation the glass fiber composites have greater fracture toughness and strength than the graphite composites. This despite the fact that the graphite fibers have a greater Young's modulus 50×10^6 psi vs. 10×10^6 psi. for the glass fibers. This is apparently due to the fact that the samples are being tested with a crack parallel to the fibers. We are thus obtaining an indication of the relative fiber to matrix bonds of the respective fibers and the results indicate a better E-glass to epoxy bond, which is consistent with the findings in Section B.

The values of the fracture parameters also indicate the crack resisting effects of fibers not aligned with the direction of crack growth. The laminated composite shows a

40 fold or greater increase in fracture toughness over unidirectional fibers. The reason is apparent since it is now required that the high strength fibers be broken if the crack is going to propagate. Near the end of the sample the fibers were of sufficient strength that the final quarter inch of the sample failed by having the laminated layers delaminate and separate except for those layers in which the fibers were aligned with the crack. Thus in this section the interlayer and intra-layer bonds broke before the fibers would fail. It is therefore apparent that designing a composite for engineering usage will involve finding an optimum combination of fiber properties, bonding strength, matrix properties, fiber orientation, and fiber volume percentage.

E. SUBCRITICAL CRACK GROWTH-FATIGUE

Fatigue tests were run on an MTS 100,000 lb. capacity testing machine. The 100 lb. Bytrex load cell was placed between the MTS grips and used to moniter loads. Loads were cycled as a sine function from a minimum of 10-12 lbs. up to a sufficient load to cause the crack to propagate. Figure 3 shows the testing arrangement.

Two 10% fiber volume specimens were successfully run. It was possible to initiate a crack from the cut notch and maintain stable crack growth in the specimens containing fibers. Fatigue tests were run at room conditions (21-23°C).

Crack lengths were measured using a transparent scale graduated in units of .05 inches attached along the lower edge of the crack. In the epoxy and 10% glass fiber volume samples it was possible to follow the crack tip using hand-held magnifying lenses. It was also found to be possible to follow the crack tip using polaroid lenses with light passed through the translucent samples. Care had to be exercised in using this method, however, since the heat from the light source was found to affect the crack growth rate. Observation of the crack tip stress field using this technique proved valuable in insuring that the true crack tip was being observed and in detecting crack branching.

Figure 19 shows the results of fatigue tests on two 10% glass fiber volume samples. Crack growth rate, $\Delta a/\Delta N$, is plotted vs. ΔG, the change in energy release rate from minimum to maximum load. Sample N-9 was run with the load cycled from 12-60 lbs. Sample N-8 was run with the load cycled from 10-50 lbs.

The N-9 growth rate increased until the critical G for the material was reached, at which time the crack growth became unstable and the sample broke,

The N-8 sample was then run at a lower load and at $a/W \approx .53$ possible crack branching was observed using the polarizing lenses and magnifying glass. This observation

was supported by the crack growth data. The growth rate dropped off at the point where branching was observed. When the growth rate again began to rise the apparent energy release rate had approximately doubled indicating two fully developed crack branches.

More work remains to be done to compare the crack growth rates for varying fiber volume fraction and to explain why the crack branching phenomenon occurred in one sample and not the other. Accurate measurement of the crack length was a problem but does not appear to be the primary factor causing the large amount of scatter in the data. This appears to be due more to the fact that the crack is propagating along the fibers and is thus highly dependent on the epoxy-fiber bond and fiber alignment.

IV. CONCLUSION

The results of the experimental testing program generally supoorted the conclusions reached in the analysis of composite systems from the conventional fracture mechanics viewpoint. It was found that the relationship between G_c and k_c for a homogeneous material in the linear elastic theory of fracture mechanics held for the glass fiber reinforced composites with a crack parallel to the fibers. The graphite fiber to epoxy matrix bond was apprarently weaker than the glass fiber to eposy matrix bond and resulted in fracture mechanisms not accounted for by the analytical model.

It was determined that a peak value of the fracture toughness, G_c, did exist for the glass fiber composites with a crack parallel to the fibers. The fiber volume percent corresponding to this peak was about 10% to 15% but the exact value could be anywhere between 0% and 20% since specimens were tested at 0, 10, 20, 50, and 60 percent. The fracture toughness at 10% fiber volume was approximately three times that found for the matrix material alone.

Tests involving a laminated graphite composite with fibers aligned with the crack and ±60° to the crack resulted in values of fracture toughness and critical crack tip stress intensity factor at least an order of magnitude greater than specimens with unidirectional fibers with the

same fiber volume. These tests indicated the crack resisting effects of fibers oriented at an angle to the preferred crack growth direction. These tests also uncovered layer delamination as an alternate or additional failure mechanism to crack propagation in this type of material.

V. FUTURE RESEARCH

The results of this experimental work indicate the need for a great deal of research to determine the optimum composite structure for engineering applications of these materials. It is obvious that practical engineering composites will require fibers to be laid at more than one orientation to resist crack growth. It is not obvious, however, what combination of orientations will provide optimum strength and fracture toughness. Testing of laminated composites with layers of various orientations would thus appear to be the next logical step.

Testing of samples with a crack in one layer should be attempted to determine the relative importance of crack growth in that layer, layer delamination, and fiber failure to the overall fracture mechanism for the material. Other areas to be explored may be layer thickness effects, woven fiber lattices vs. unidirectional fiber layers, and optimum ratios of fibers in each orientation for various loading situations.

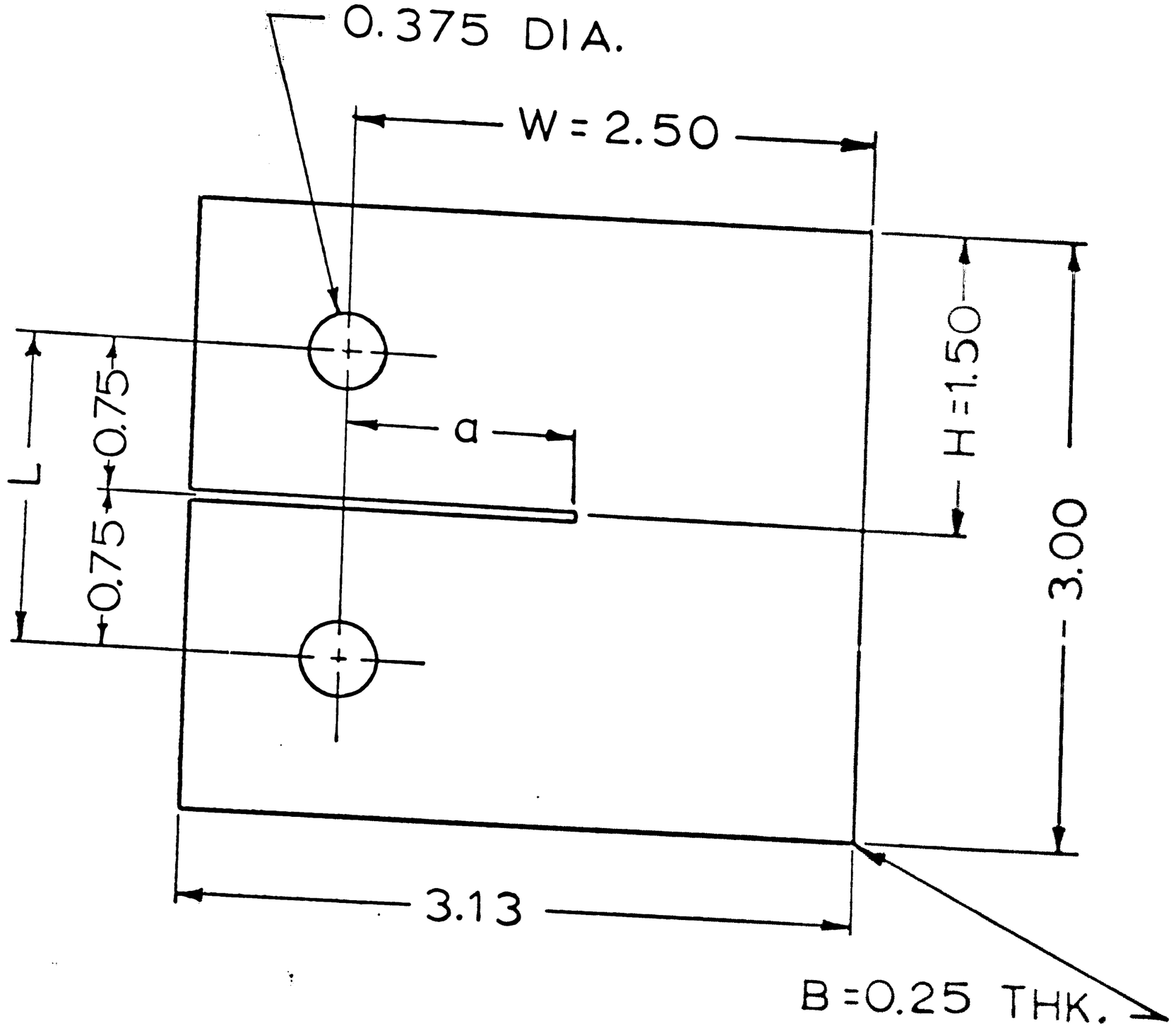

COMPACT TENSION SPECIMEN

Figure 1

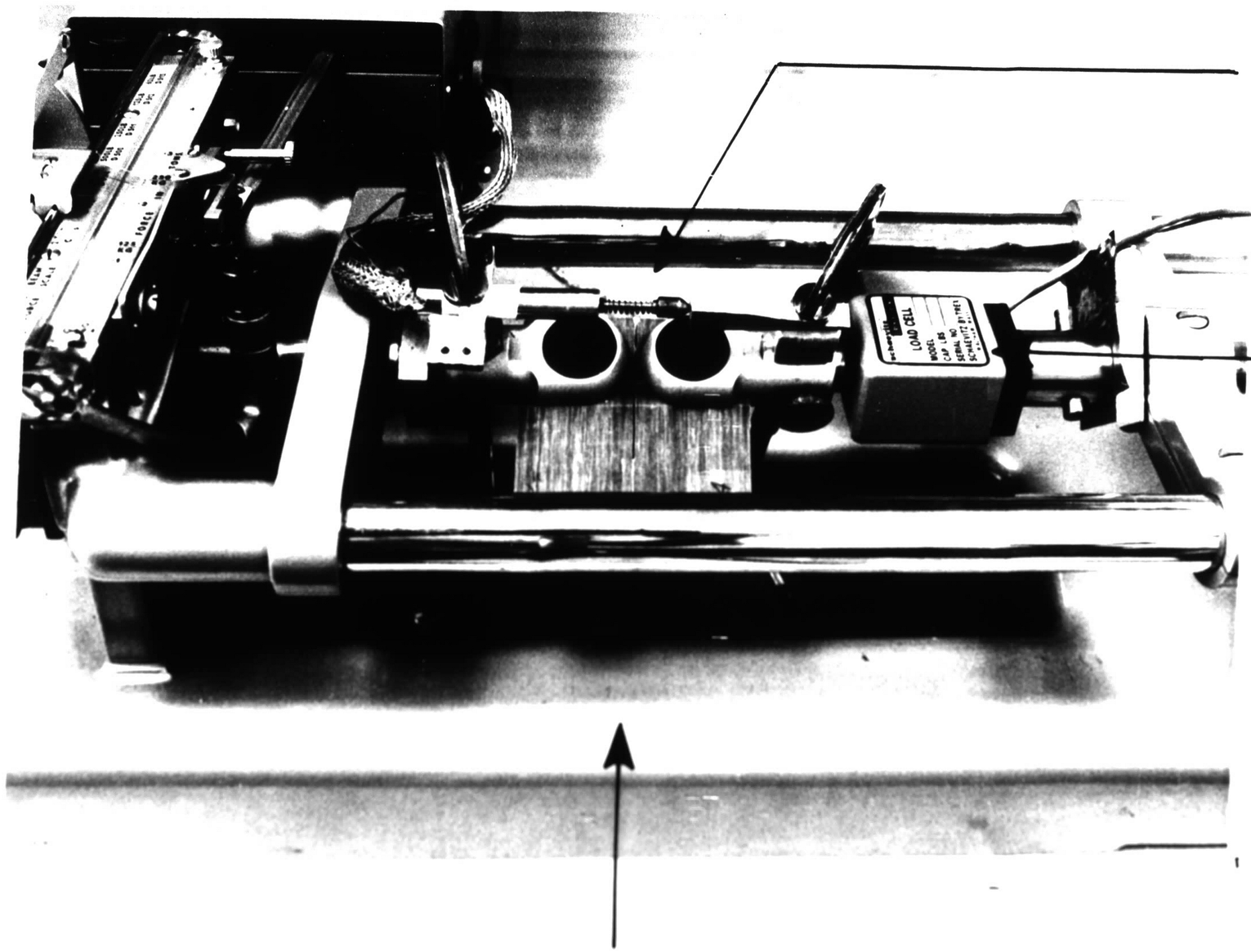

Figure 2 Testing Arrangement for Compliance and Fracture Test.

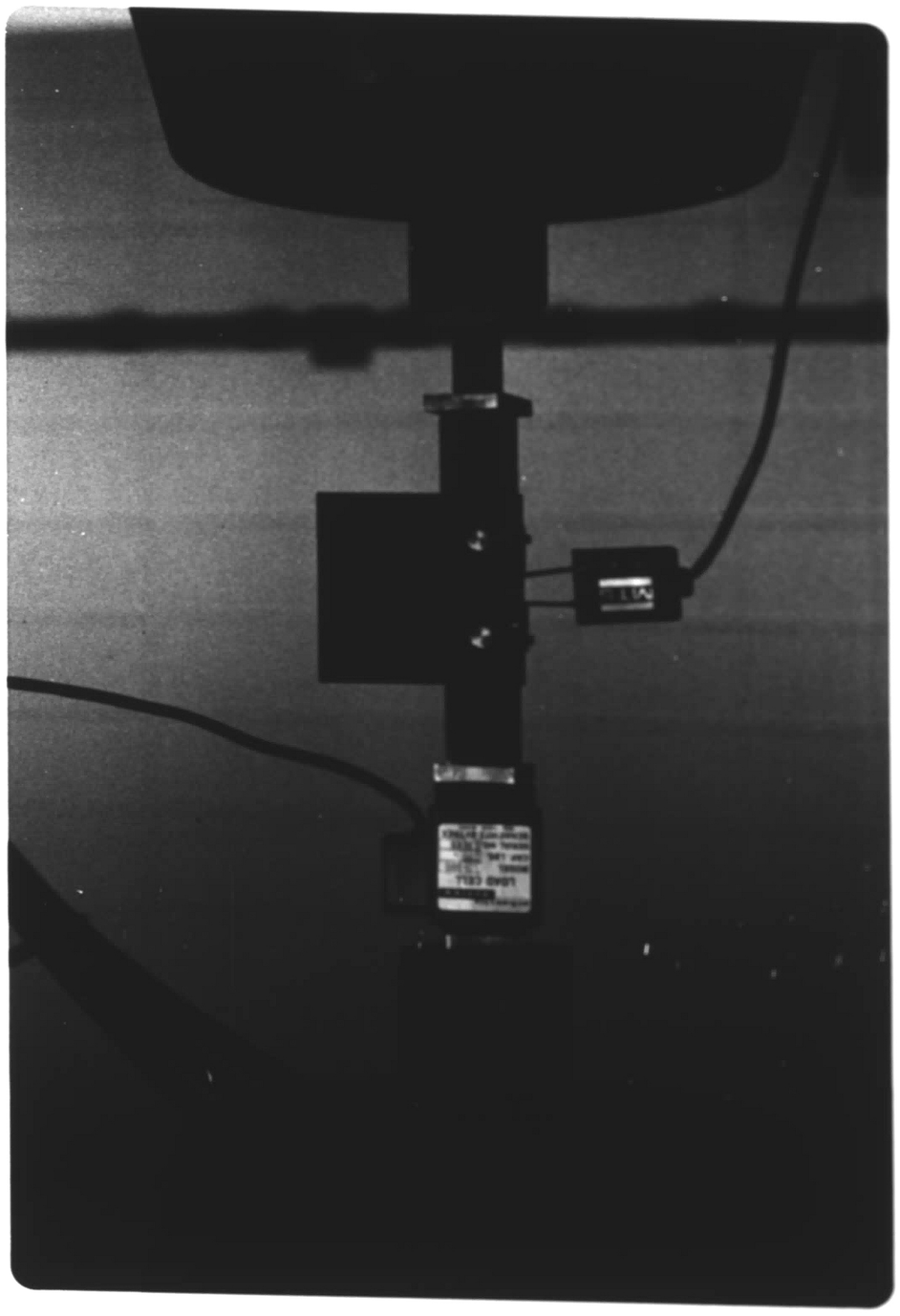

Figure 3 Testing Arrangement for Fatigue Tests.

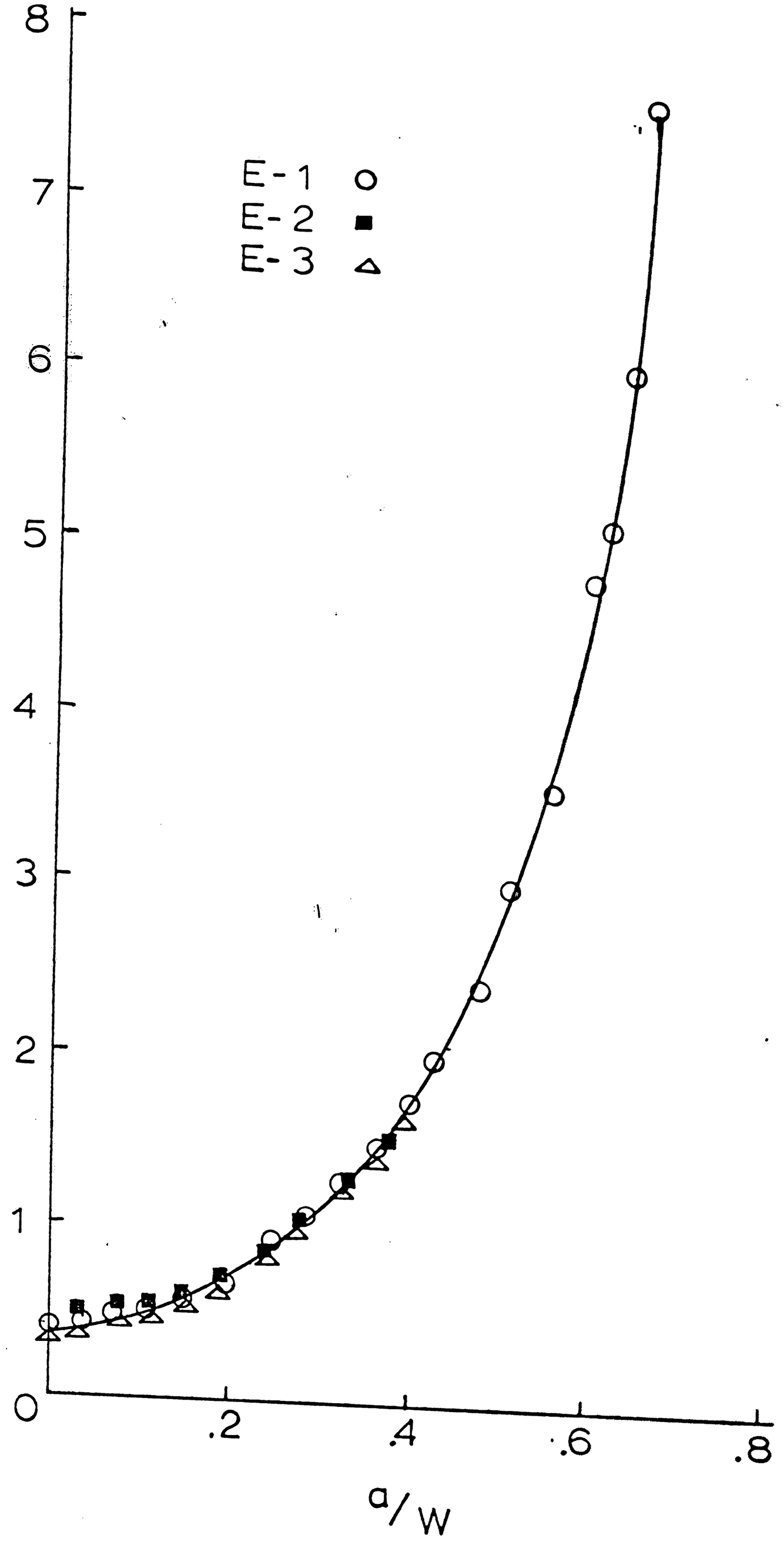

Figure 4 Compliance Calibration Curve for 0% Fiber Volume

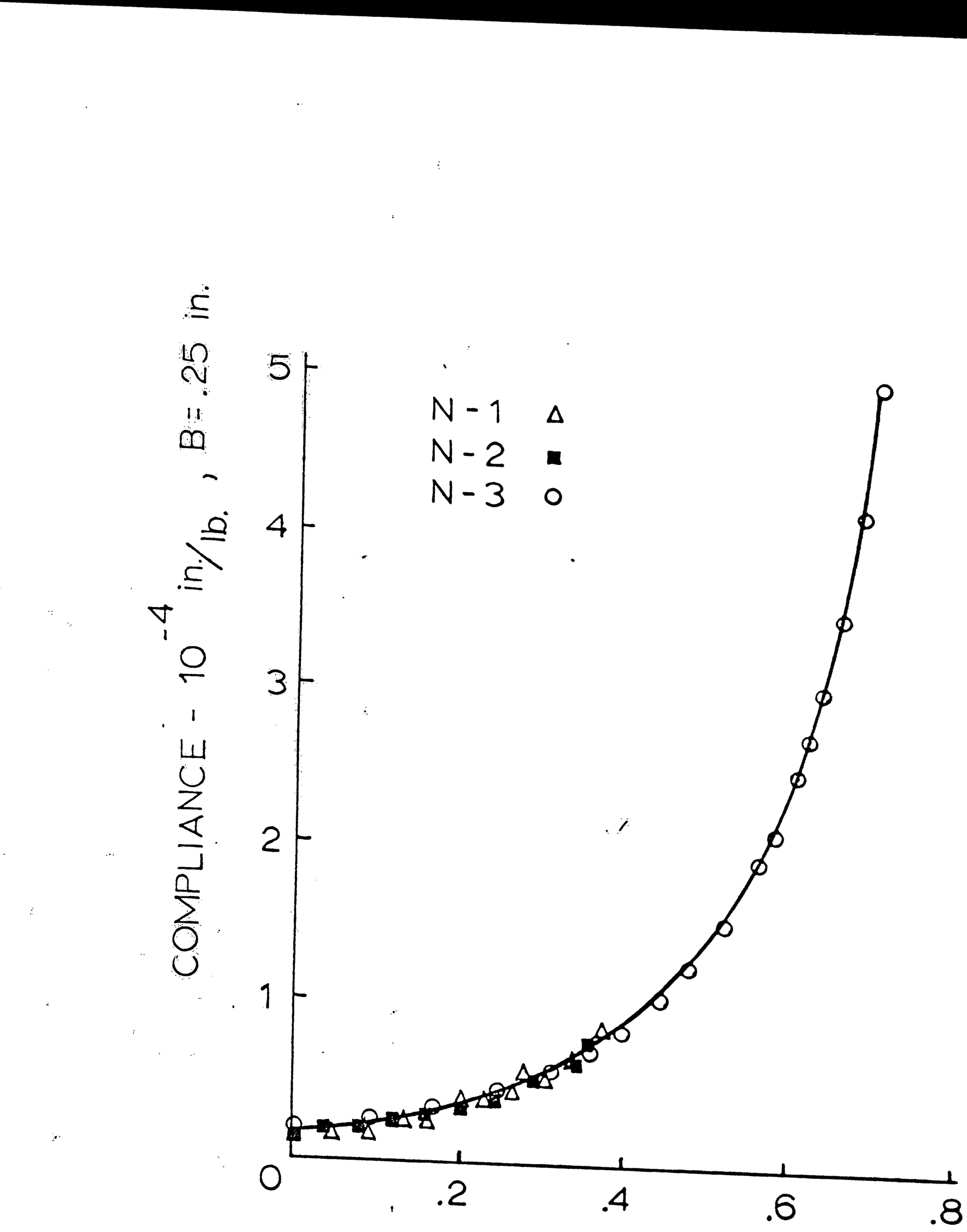

Figure 5 Compliance Calibtation Curve for 10% Unidirectional Glass Fiber Volume.

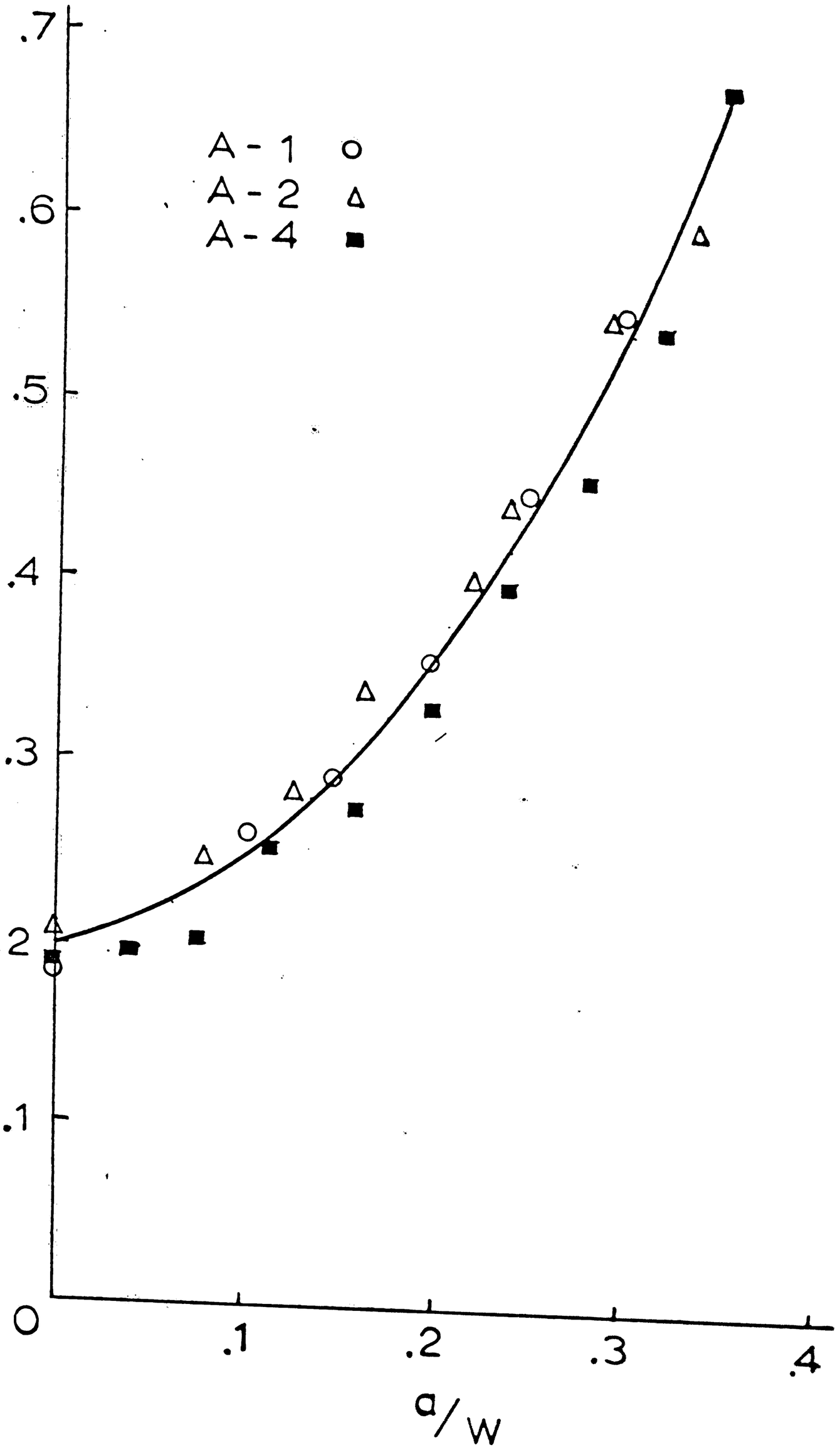

Figure 6 Compliance Calibration Curve for 20% Unidirectional Glass Fiber Volume.

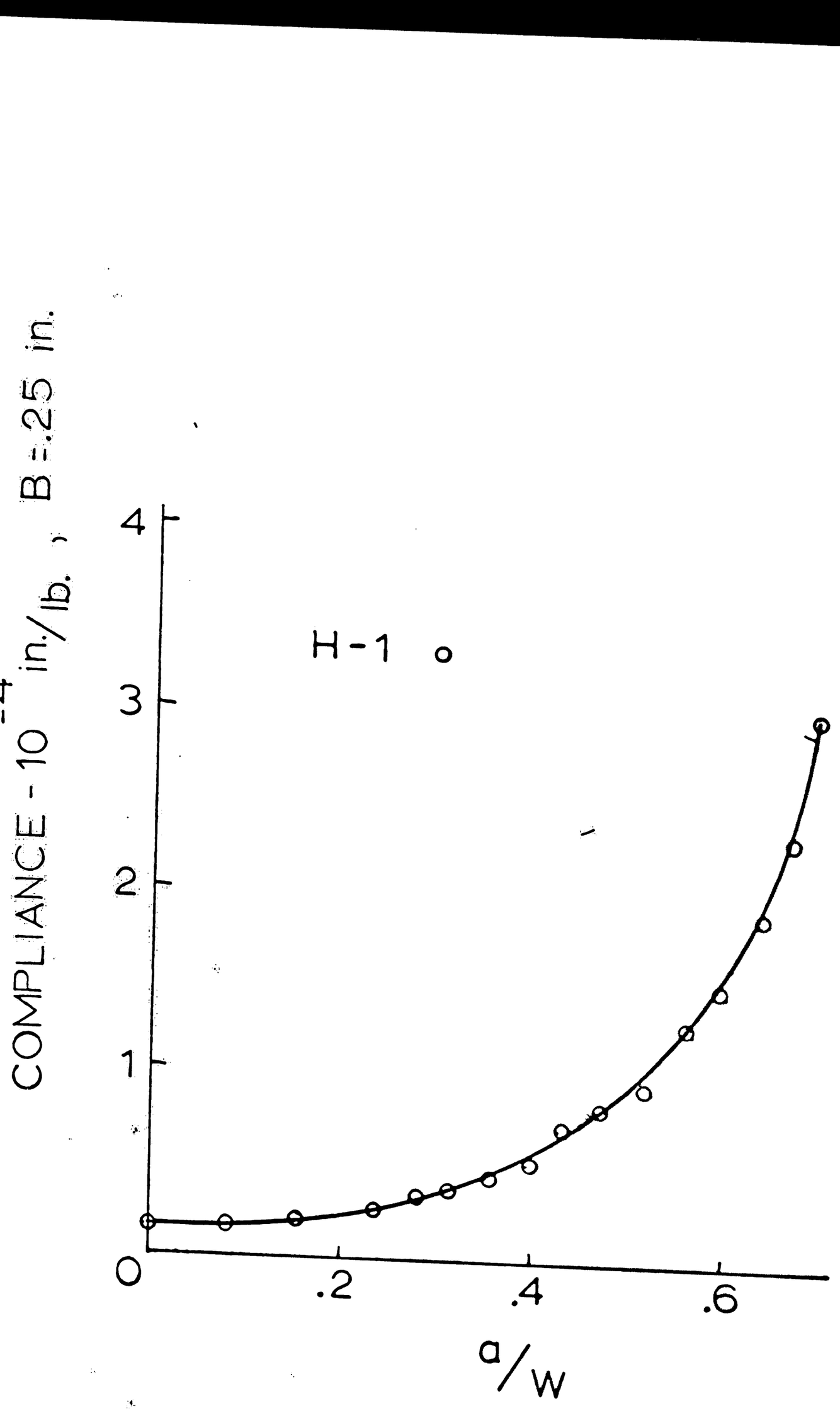

Figure 7 Compliance Calibration Curve for 50-55% Unidirectional Glass Fiber Volume.

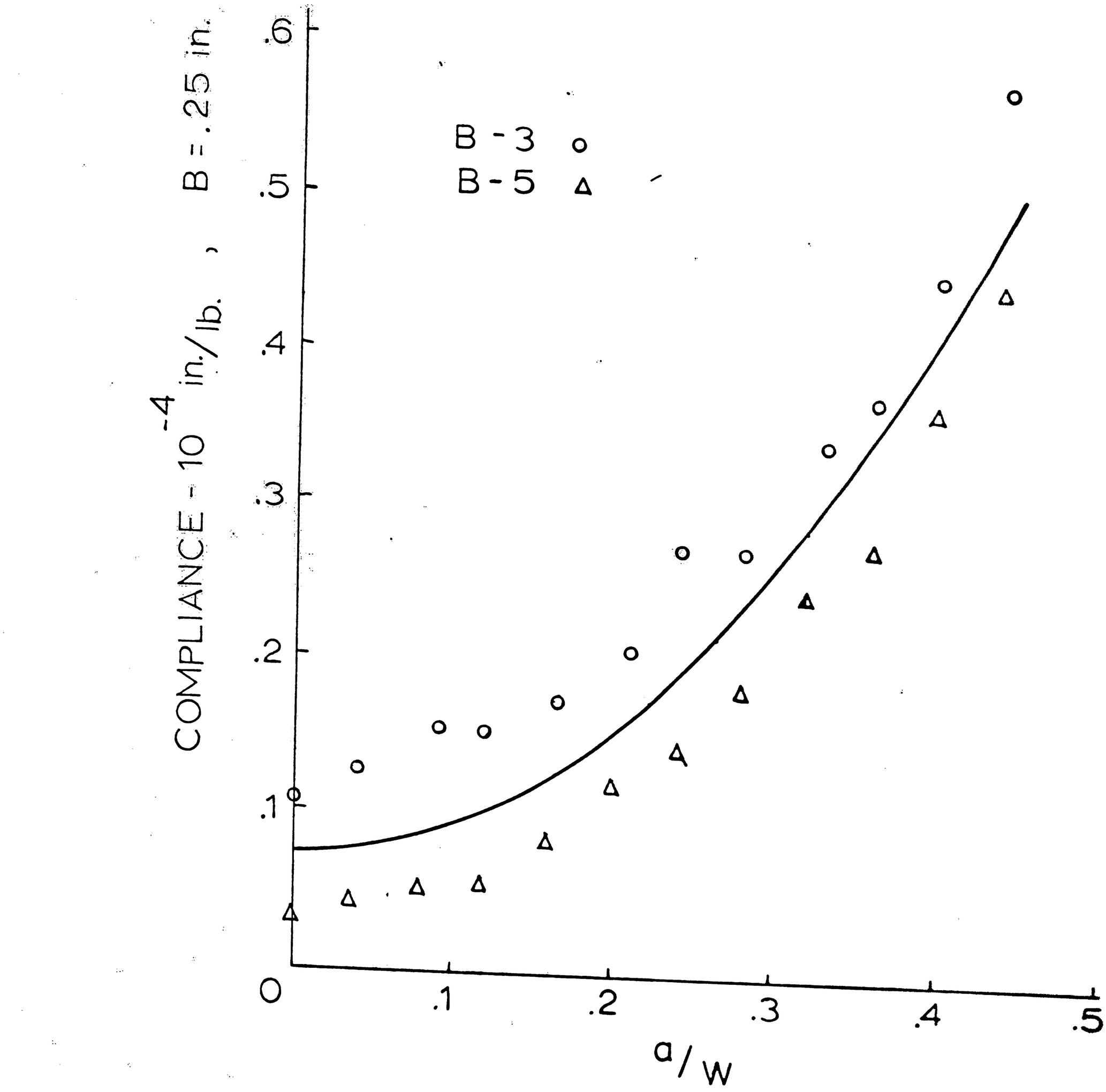

Figure 8 Compliance Calibration Curve for 60% Unidirectional Glass Fiber Volume.

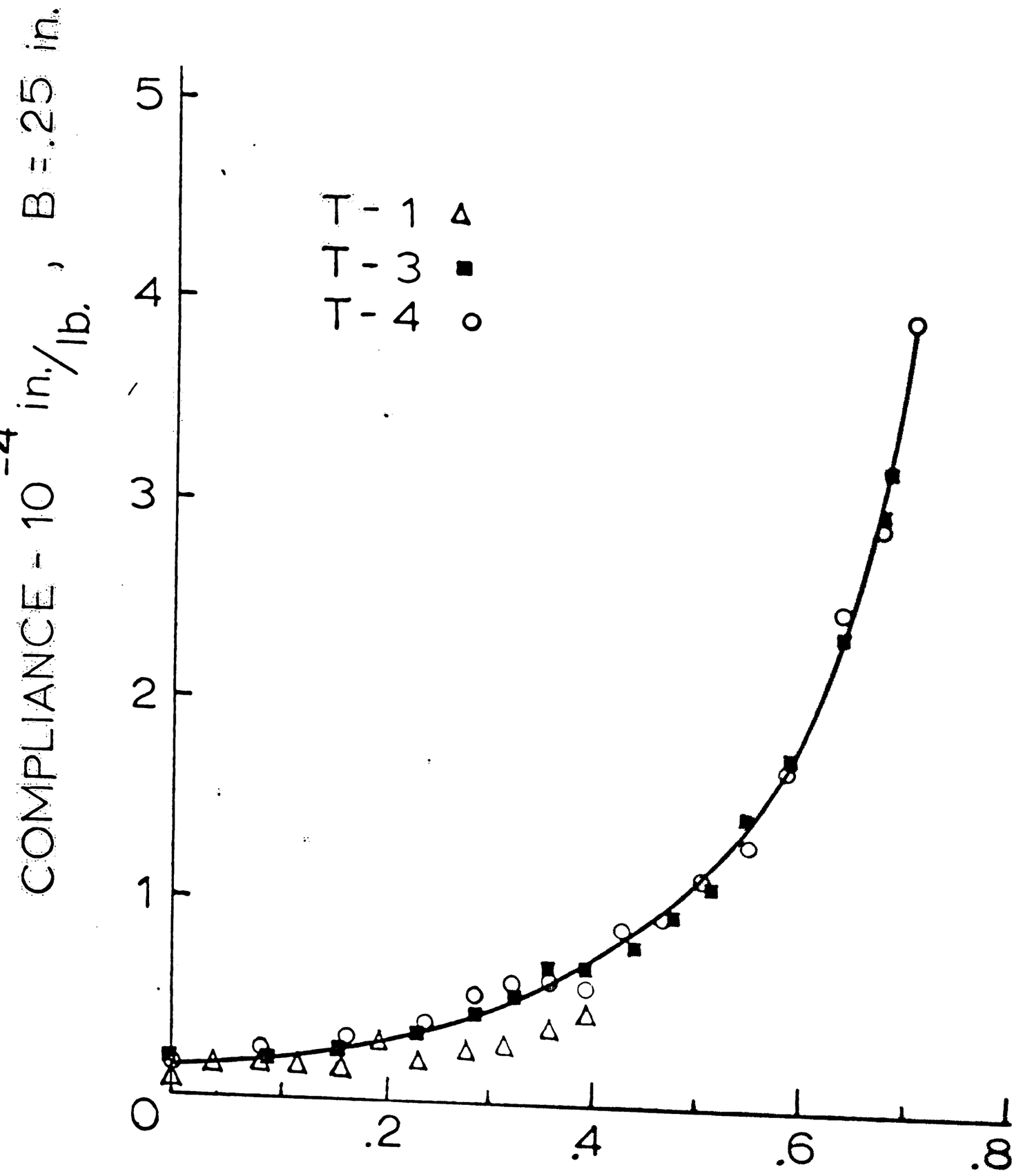

Figure 9 Compliance Calibration Curve for 50-55% Unidirectional Graphite Fiber Volume.

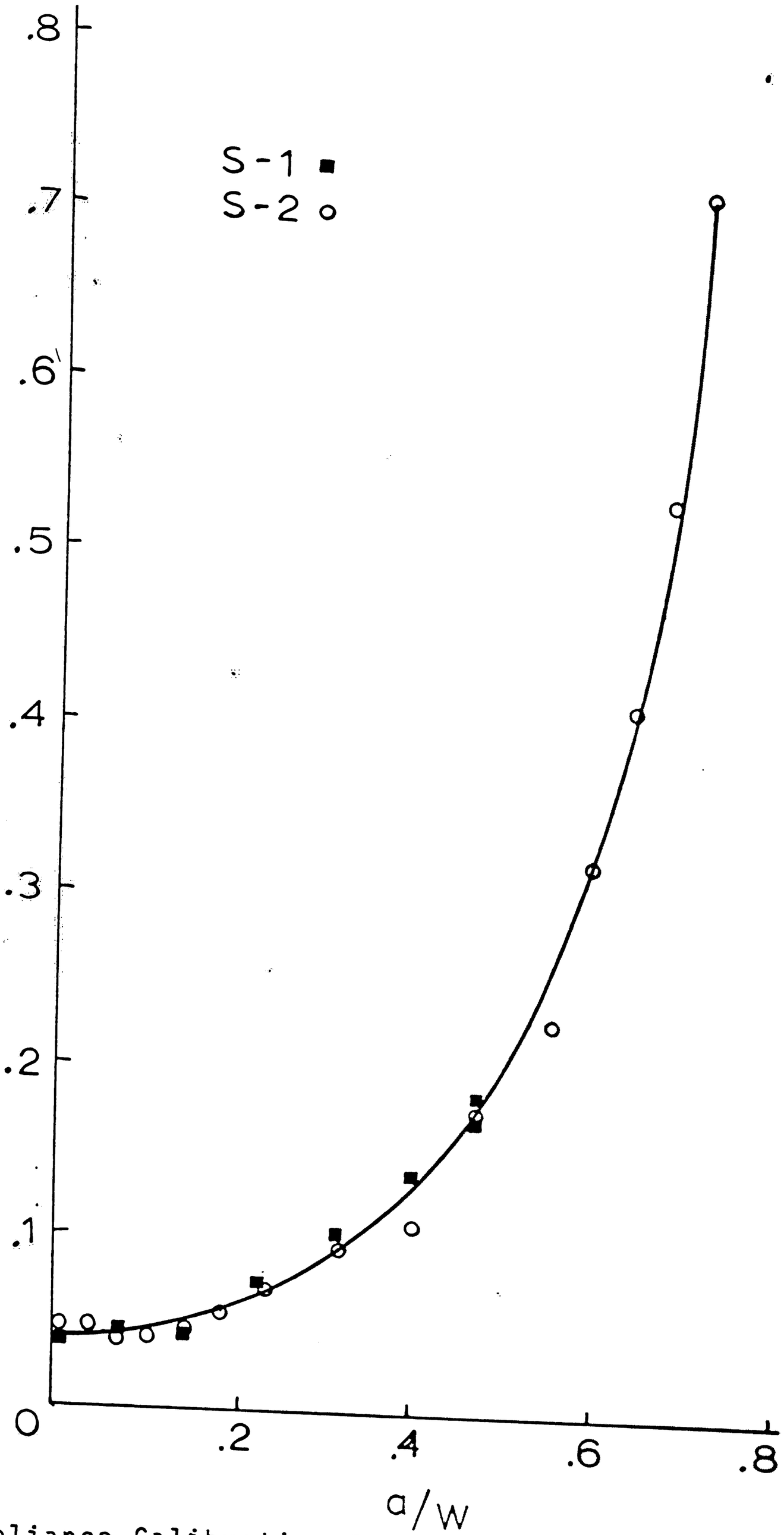

Figure 10 Compliance Calibration Curve for 50-55% Laminated 0°, ±60° Graphite Fiber Volume.

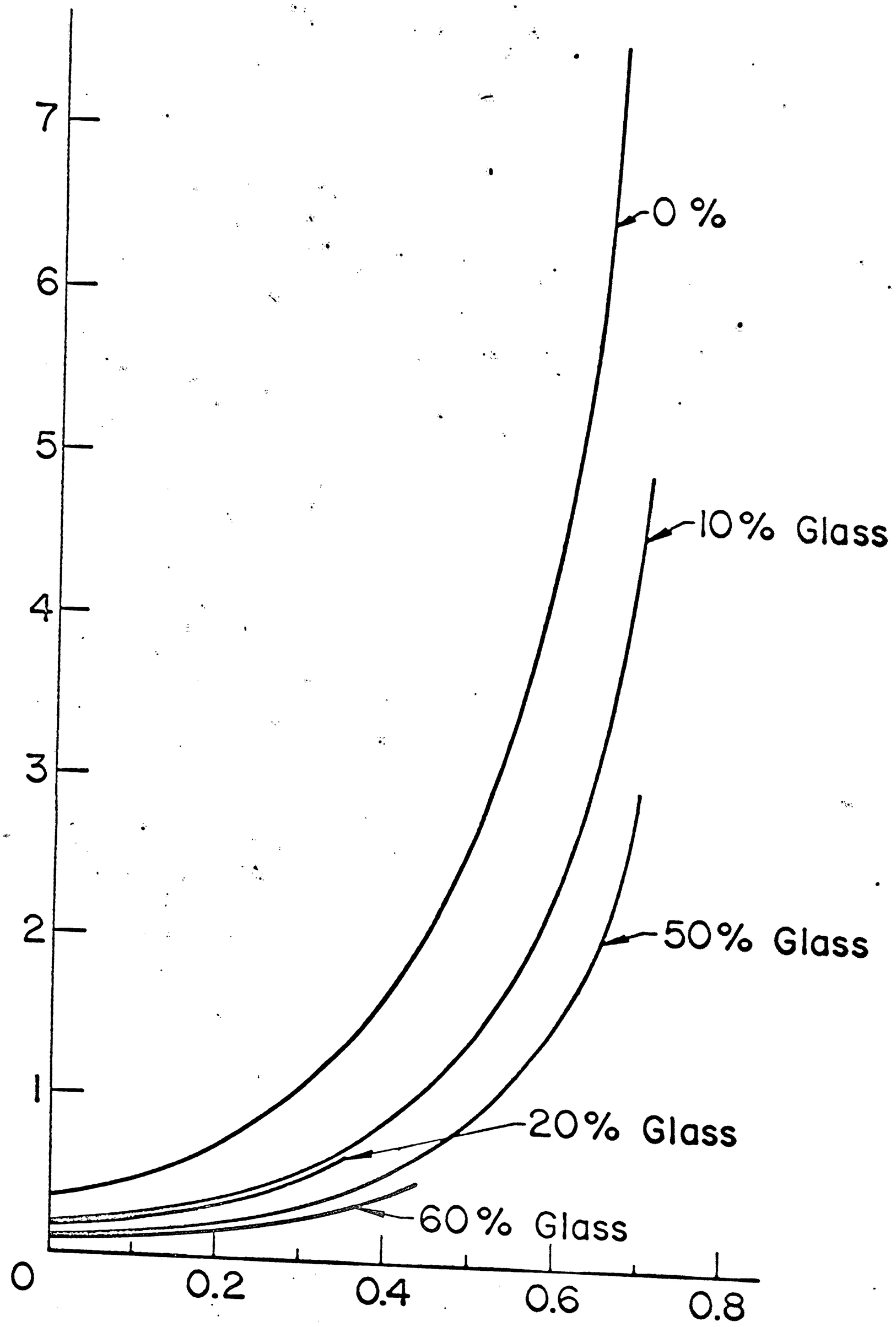

Figure 11 Comparison of Glass Fiber Calibration Curves.

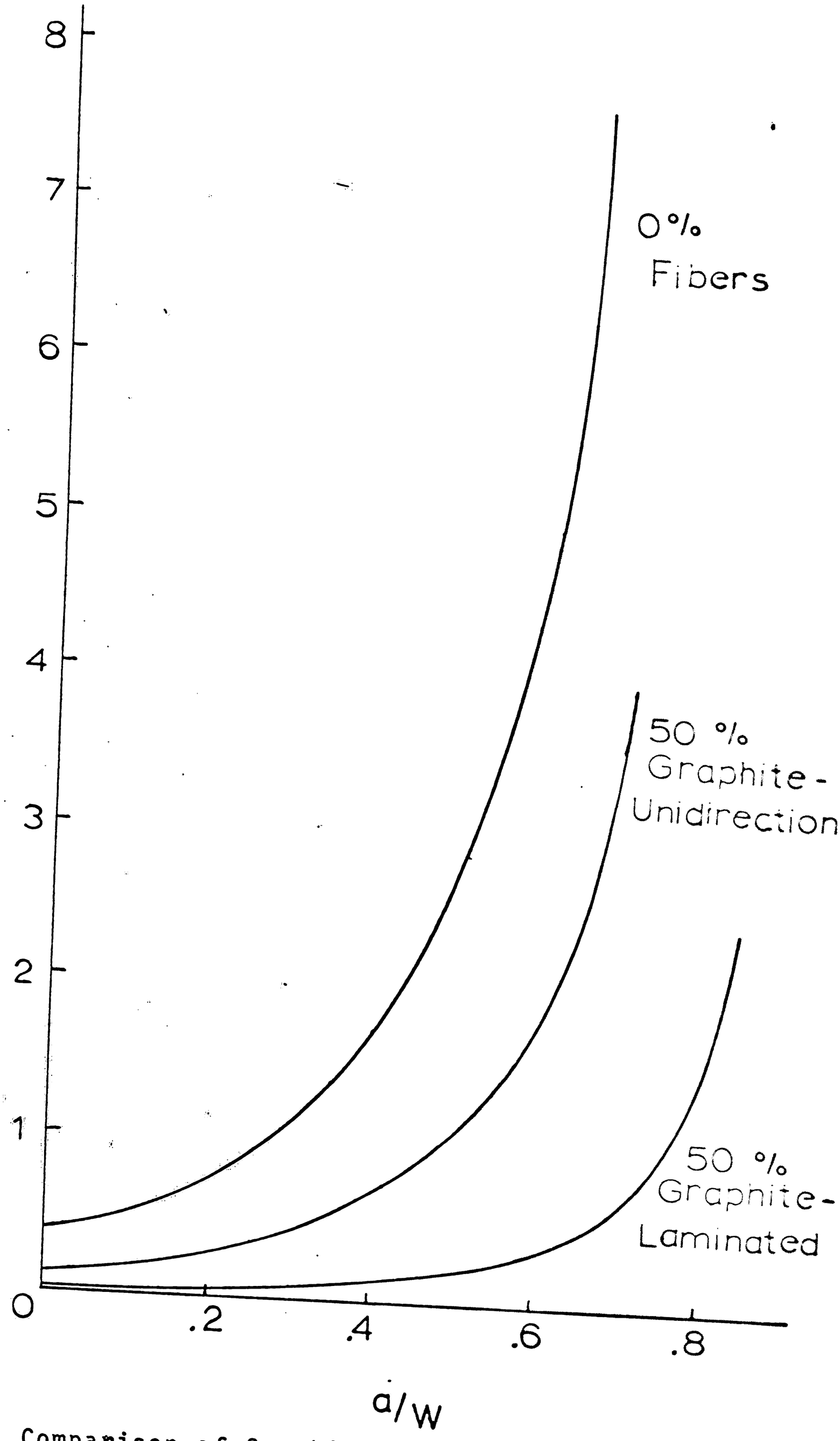

Figure 12 Comparison of Graphite Fiber Calibration Curves.

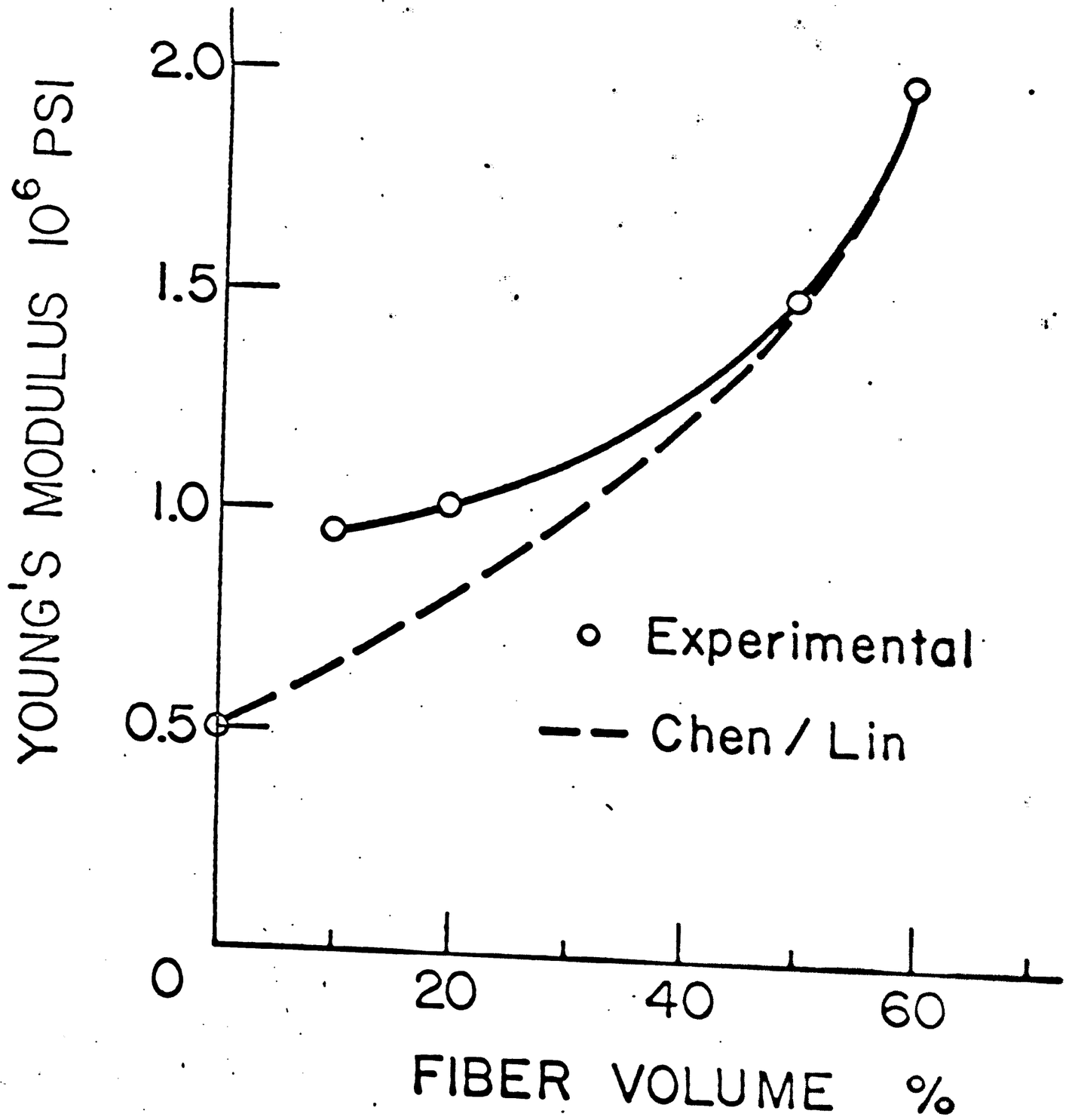

Figure 13 Comparison of Experimental Young's Modulus with Chen and Lin's Results.

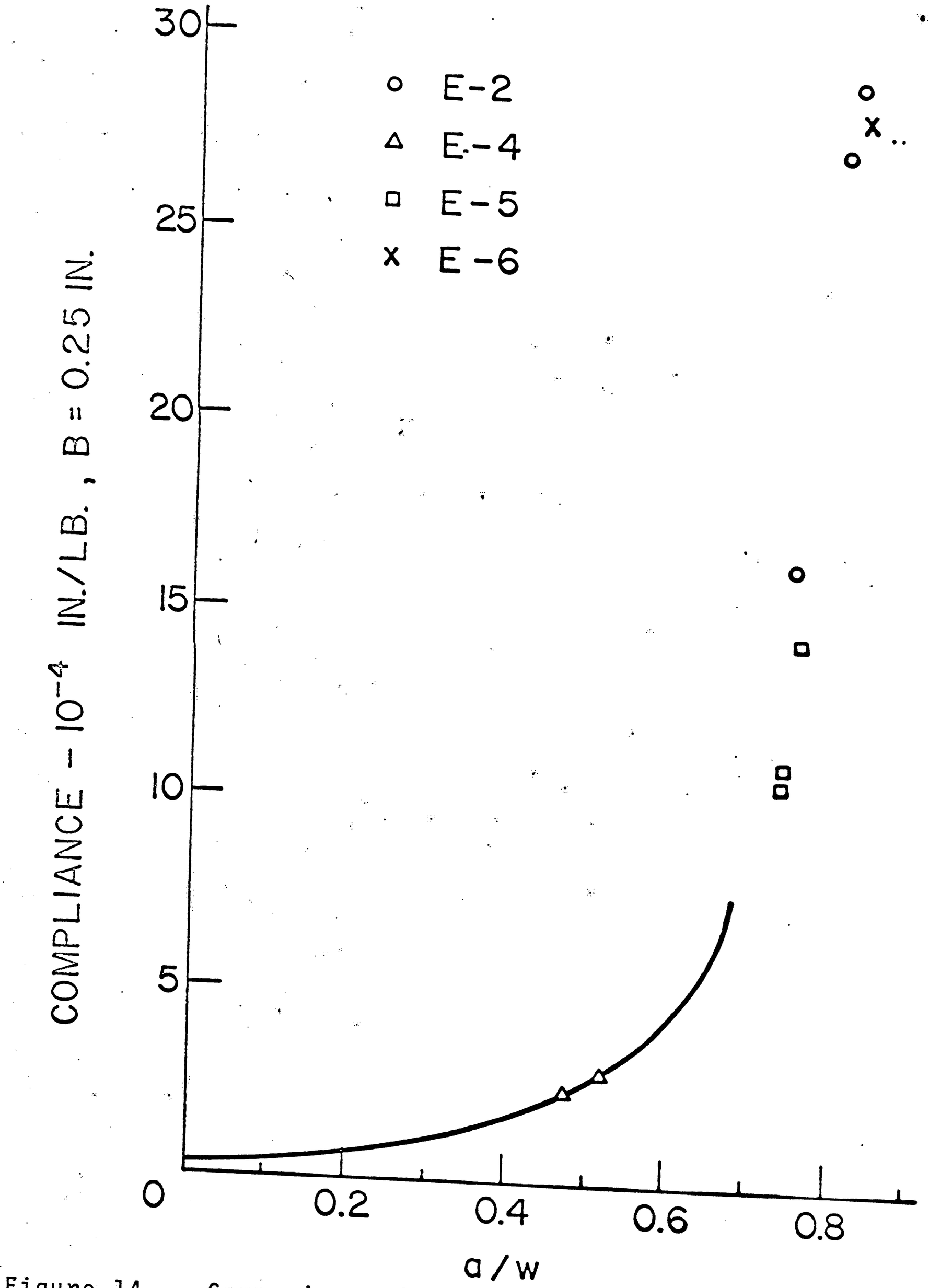

Figure 14 Comparison of Compliance Calibration Curve With Compliance for Fracture Specimen for Epoxy Resin Matrix Material.

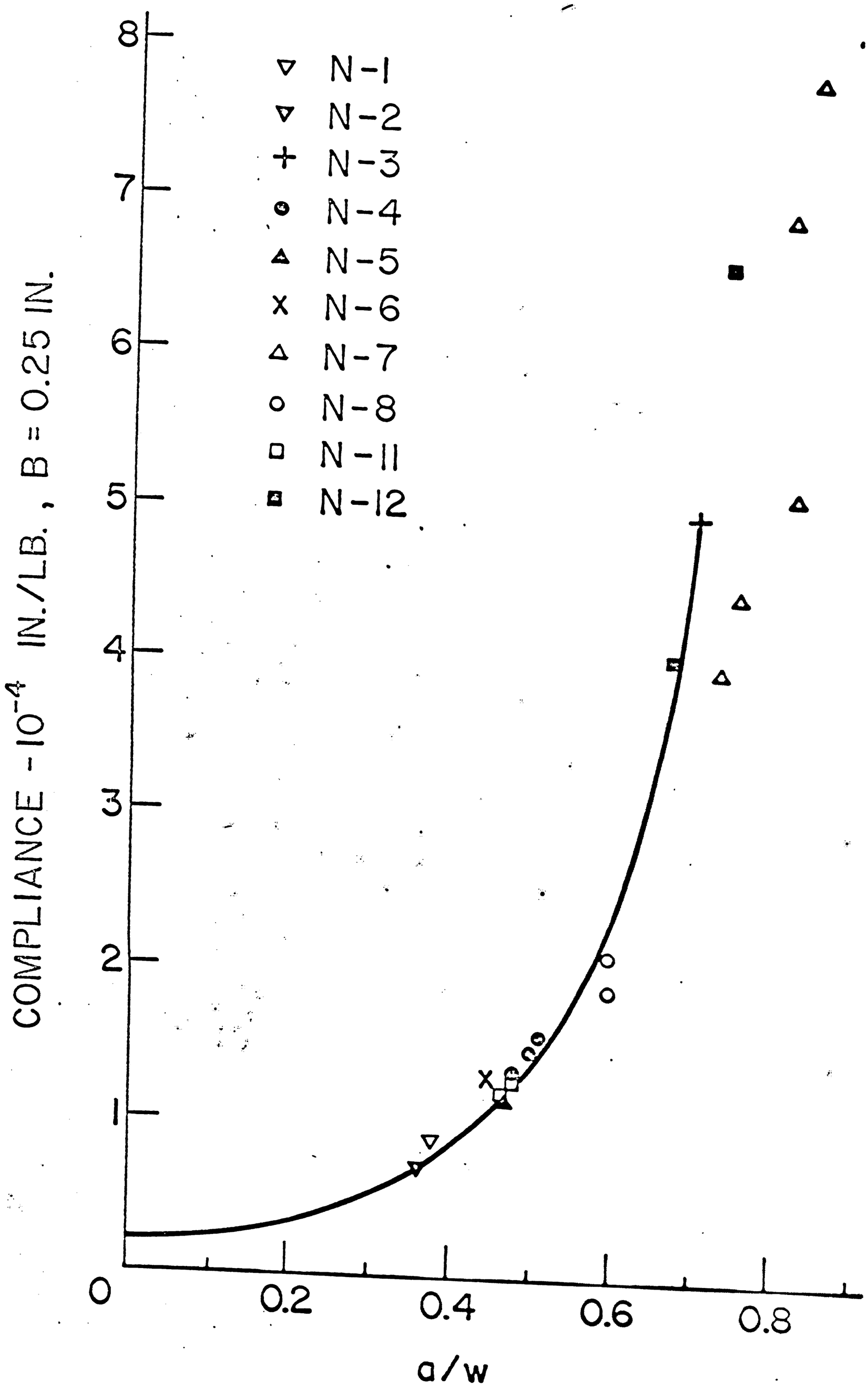

Figure 15 Comparison of Compliance Calibration Curve With Compliance for Fracture Specimen for 10% Unidirectional Glass Fiber Volume.

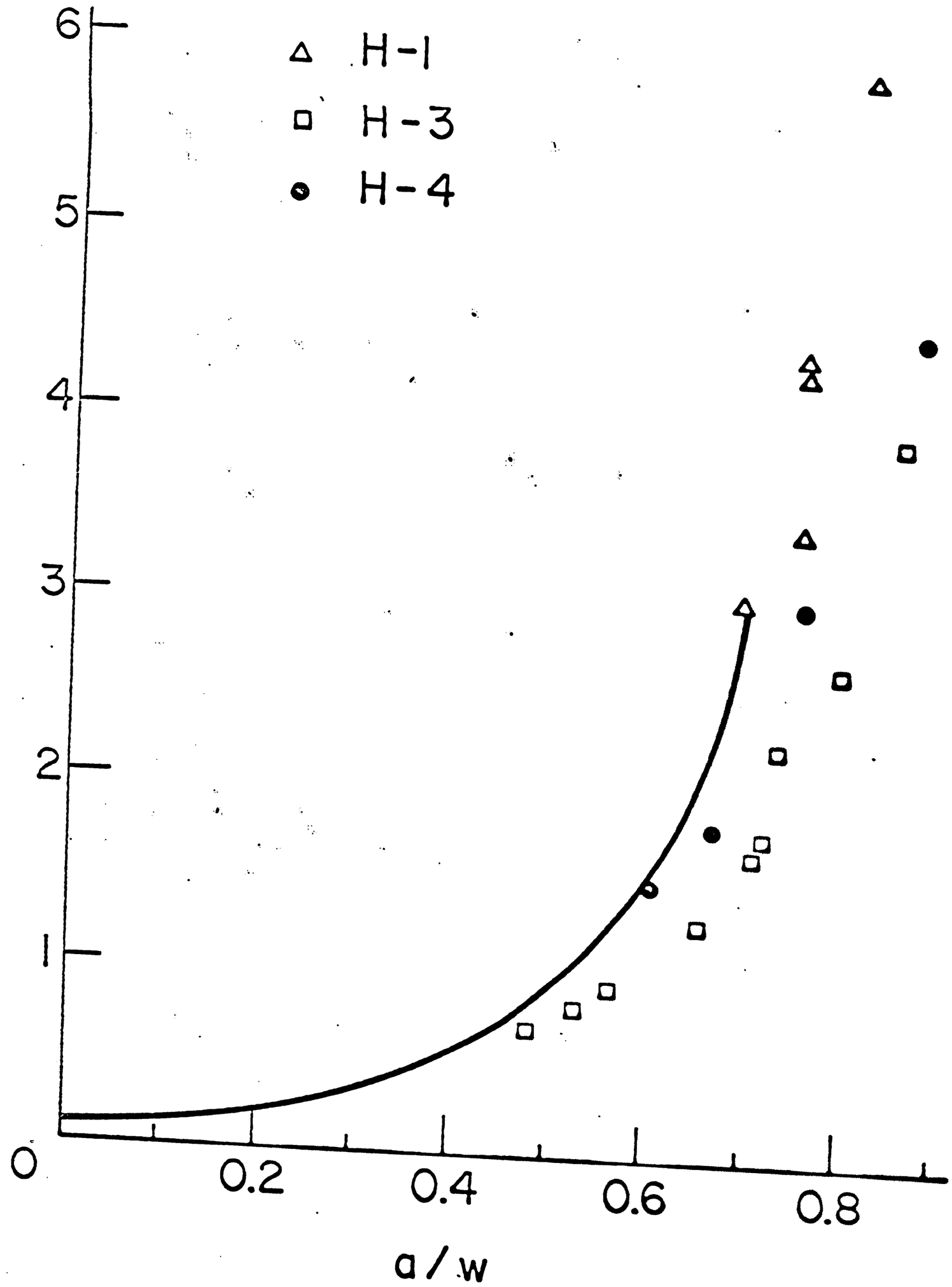

Figure 16 Comparison of Compliance Calibration Curve With Compliance for Fracture Specimen for 10% Unidirectional Glass Fiber Volume.

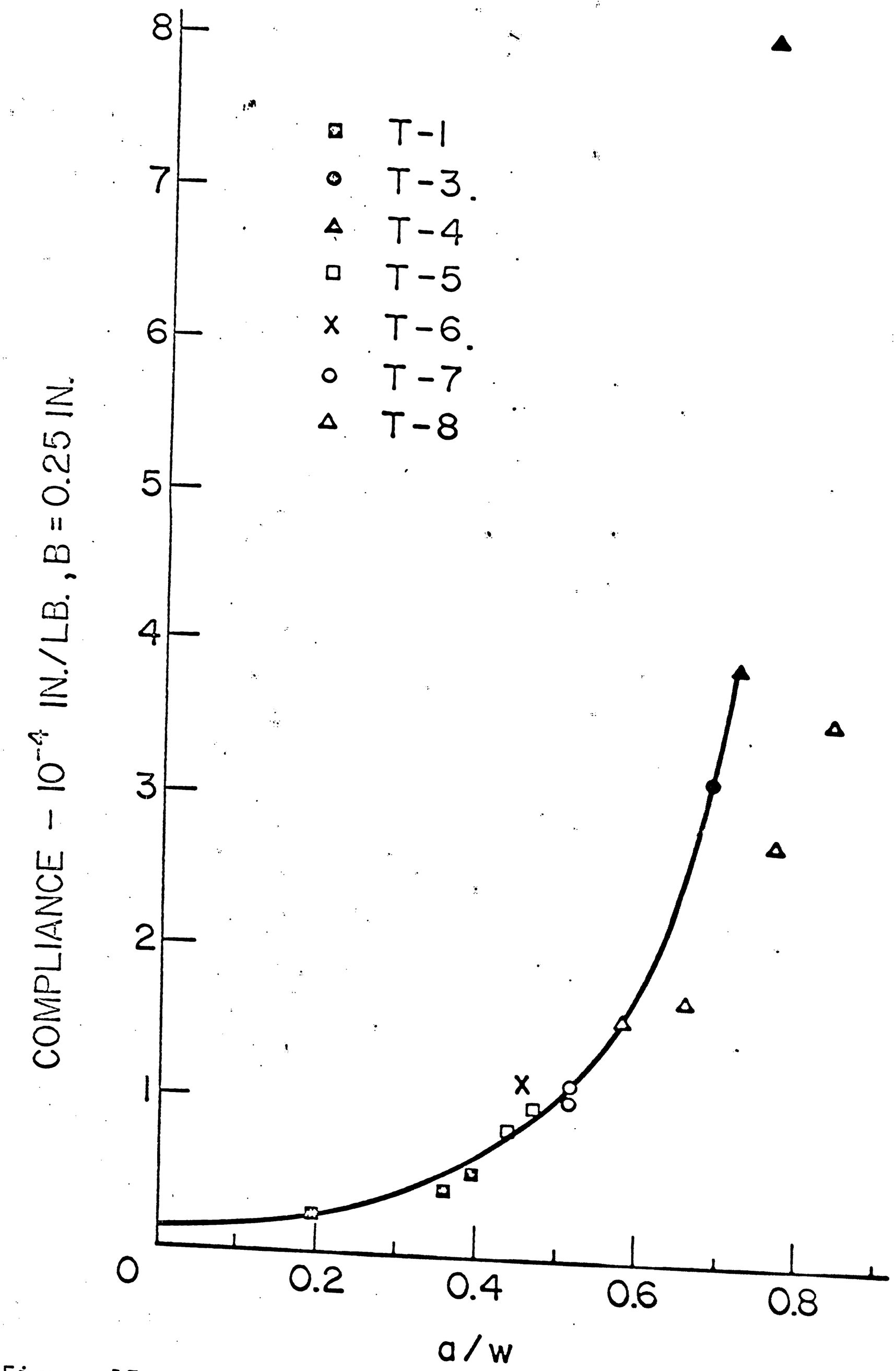

Figure 17 Comparison of Compliance Calibration Curve With Compliance for Fracture Specimen for 50-55% Unidirectional Graphite Fiber Volume.

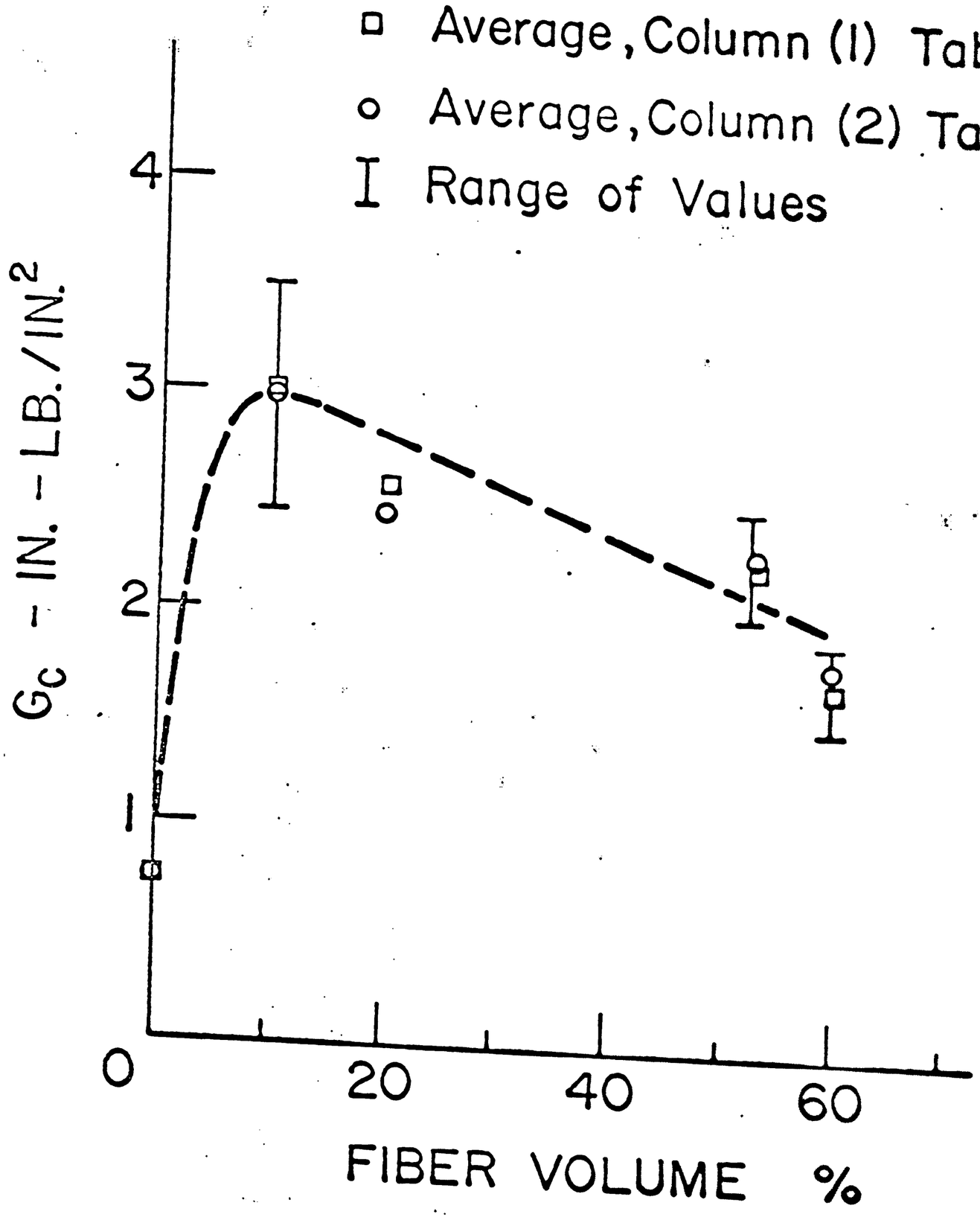

Figure 18 Fracture Toughness, G_c vs. Fiber Volume Percent for Unidirectional Glass Fibers in Compact Tension Specimen.

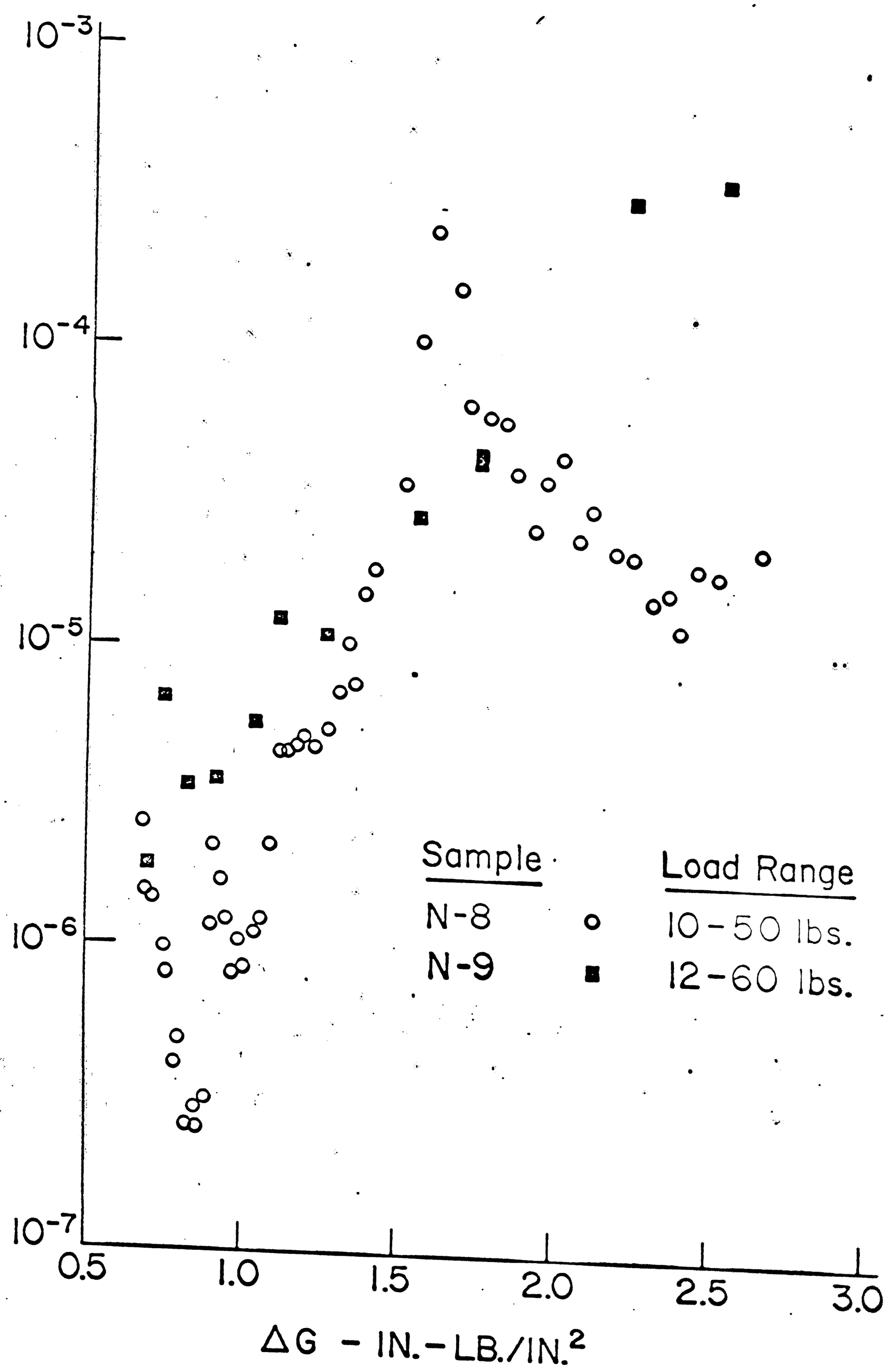

Figure 19 Crack Growth Rate vs. Fracture Toughness for 10% Glass Fiber Volume Compact Ension Specimen with Unidirectional Fibers.

REFERENCES

[1] Adams, D. F., and Doner, D. R., "Transverse Loading of a Unidirectional Composite", Journal of Composite Materials, Vol. 1, April 1967, pp. 152-163.

[2] Adams, D. R., and Tsai, S. W., "The Influence of Random Filament Packing of the Transverse Stiffness of Unidirectional Composites", Journal of Composite Materials Vol. 3, July 1969, pp. 368-381.

[3] Chen, C. H. and Cheng, Shan, "Mechanical Properties of Fiber Reinforced Composites", Journal of Composite Materials, Vol. 1, Jan. 1967, pp. 30-41.

[4] Chen, P. E., and Lin, J. M., "Transverse Properties of Fibrous Composites", Materials Research and Standards, MTRSA, Vol. 9, No. 8, pp. 29-33.

[5] Hertzberg, R. W., Manson, J. A., and Nordberg, H., Fatigue Crack Propagation in Resin-Fiber Composites, Technical Report AFML-TR-69-92, November 1969.

[7] Sih, G. C., Hilton, P. D., and Wei, R. P., Exploratory Development of Fracture Mechanics of Composite Systems, Technical Report AFML-TR-70-112, June 1970.

[8] Sih, G. C., Hilton, P. D., Badaliance, R., Shenberger, P. S., and Villarreal, G., Fracture Mechanics Studies of Composite Systems, Technical Report AFML-TR-70-? June 1971.

[9] Parikh, N. M., "Deformation and Fracture Modes in Fiber Composite Materials, ASM publication of seminar papers, 1965, pp. 115-130.

[10] Brown, W. R. Jr., and Srawley, J. E., Plane Strain Crack Toughness Testing of High Strength Metallic Materials, ASTM Special Technical Publication No. 410, 1966, pp. 1-15.

[11] Sih, G. C. and Liebowitz, H.,"Mathematical Theories of Brittle Fracture", Mathematical Fundamentals of Fracture, Edited by H. Liebowitz, Vol. 2, Academic Press, New York, 1968, pp. 67-190.

VITA

Paul Sidney Shenberger, the son of Paul S. and Hilda R. Shenberger was born December 18, 1946, in Lancaster, Pennsylvania. He attended public schools in New Holland, Pa. and graduated from Garden Spot High School in June 1964.

The Author entered Drexel Institute of Technology in September, 1964 and was awarded the degree of Bachelor of Science in Mechanical Engineering in June 1969. While in the cooperative engineering program at Drexel he spent a total of 2 years in the Engineering Division at New Holland Division of Sperry Rand Corporation.

He began graduate study at Lehigh University in September 1969 under an N.D.E.A. Fellowship and expects to be awarded the Master of Science degree in Applied Mechanics in October, 1971.